SPACE SCIENCES

Early scattering of the solar protoplanetary disk recorded in meteoritic chondrules

Yves Marrocchi,[1]* Marc Chaussidon,[2] Laurette Piani,[3] Guy Libourel[4]

Meteoritic chondrules are submillimeter spherules representing the major constituent of nondifferentiated planetesimals formed in the solar protoplanetary disk. The link between the dynamics of the disk and the origin of chondrules remains enigmatic. Collisions between planetesimals formed at different heliocentric distances were frequent early in the evolution of the disk. We show that the presence, in some chondrules, of previously unrecognized magnetites of magmatic origin implies the formation of these chondrules under impact-generated oxidizing conditions. The three oxygen isotopes systematic of magmatic magnetites and silicates can only be explained by invoking an impact between silicate-rich and ice-rich planetesimals. This suggests that these peculiar chondrules are by-products of the early mixing in the disk of populations of planetesimals from the inner and outer solar system.

INTRODUCTION

Planetary systems are ubiquitous across the galaxy (1), revealing the efficiency of dust formation and agglomeration around stars during their first million years of evolution. In our solar system, the formation of pebbles by gravitational instabilities in regions with high dust/gas ratios could have induced the rapid accretion of 1000-km planetesimals in a few orbital periods (2). Hydrodynamic simulations also indicate that the early formation of giant planets likely induced collisions between planetesimals formed at different heliocentric distances in the solar accretion disk (3). Primitive meteorites (chondrites) are the only available fragments of asteroidal belt objects that formed early in the disk and escaped global melting and differentiation. Chondrites comprise four main components: refractory inclusions [Ca-Al–rich inclusions (CAIs)], chondrules, Fe-Ni metal beads, and fine-grained matrix. CAIs and chondrules experienced a complicated high-temperature history as isolated grains in the disk before their accretion into planetesimals; they therefore provide key constraints on the evolving dynamics and physicochemical conditions of the accretion disk.

Chondrules are submillimeter silicate-rich spherules mainly composed of olivine (Mg_2SiO_4), low-Ca pyroxene ($MgSiO_3$), glassy mesostasis, and Fe-Ni metal beads and commonly contain iron sulfide (FeS) and magnetite (Fe_3O_4) (4). The mineralogy, textures, and chemistry of chondrules suggest that they formed by incomplete melting (that is, 1400° to 1750°C) of solids with likely cooling rates varying between 10 and 1000 K·hour^{-1} (5). After decades of investigations, the origin of the chondrule precursors and the nature and location of the chondrule-forming event(s) remain highly debated. Two scenarios are generally considered: (i) a nebular origin in which chondrules result from shock waves propagating through a dusty nebular gas [for example, (5)] and (ii) a planetary origin for chondrules in which chondrule formation was induced by planetary type collisions (6) or related to bow shocks produced by planetary embryos (7). Recent advances based on reconstruction of the partial pressure of volatile elements surrounding the melted chondrules (8–10) suggest noncanonic high pressures as could be produced by dust evaporation in regions of the disk with high dust/gas ratios or

by impacts between planetary objects. However, the redox state of the gas with which the chondrules equilibrated has not been quantified precisely and would provide important constraints on the nature of the chondrule-forming event and the dynamics of the protoplanetary disk.

RESULTS

Here, we report the presence of previously unrecognized sulfide-associated magnetites (SAMs) of magmatic origin (Fig. 1, fig. S1, and table S1) in chondrules from the weakly metamorphosed CV3 chondrites Vigarano and Kaba (that is, 3.1 and 3.1 to 3.4, respectively). Among the 96 Mg-rich porphyritic type I chondrules examined in two sections of Kaba and Vigarano, all chondrules present sulfides in close associations with magnetite (Fig. 1 and fig. S1). Twenty-one chondrules that present magnetites of sufficient size for petrographic and isotopic analyses were chosen for detailed characterization. SAMs exhibit varying morphologies, from ameboidal droplets to large interstitial pools that partially, or totally, enclose low-Ca pyroxenes and/or olivines (Fig. 1). SAMs are Cr-free and devoid of Fe-Ni metal in contrast to magnetite observed in opaque assemblages (OAs; Fig. 1).

Oxygen isotopic compositions are expressed in δ units, or deviations in parts per thousand (‰) of the $^{17}O/^{16}O$ and $^{18}O/^{16}O$ ratios relative to a standard [here, Standard Mean Ocean Water (SMOW)], according to the equation $\delta^{17,18}O = [(^{17,18}O/^{16}O)_{sample}/(^{17,18}O/^{16}O)_{SMOW} - 1] \times 1000$. Samples related by mass fractionation to the composition of SMOW fall on a line with a slope of 0.52 due to mass differences between oxygen isotopes [terrestrial fractionation line (TFL)], whereas mass-independent variations are described by the parameter $\Delta^{17}O$, defined as $\Delta^{17}O = \delta^{17}O - 0.52 \times \delta^{18}O$ (representing deviation from the TFL). In our samples, olivine oxygen isotopic compositions plot along the carbonaceous chondrite anhydrous mineral line, with $\delta^{17}O$ and $\delta^{18}O$ ranging from −8.2 to −6.0‰ and from −5.2 to −1.8‰, respectively (Fig. 2 and table S2). SAMs present distinct oxygen isotopic compositions with low variability within each chondrule (that is, σ ≤ 1.5‰; table S2) and falling close to the Young and Russell (YR) line (Fig. 2), with $\delta^{17}O$ and $\delta^{18}O$ ranging from −6.0 to +1.8‰ and from −5.0 to +3.3‰, respectively (11). The $\Delta^{17}O$ of SAMs and coexisting olivines do not overlap; they define discrete domains from −3.7 and +0.1‰ and from −5.7 to −4.9‰, respectively (table S2).

[1]Centre de Recherches Pétrographiques et Géochimiques, CNRS, Université de Lorraine, UMR 7358, 54501 Vandoeuvre-lès-Nancy, France. [2]Institut de Physique du Globe de Paris, Université Sorbonne Paris Cité, 75238 Paris, France. [3]Department of Natural History Sciences, Hokkaido University, Sapporo 060-0810, Japan. [4]Observatoire de la Côte d'Azur, CS 34229, 06304 Nice, France.
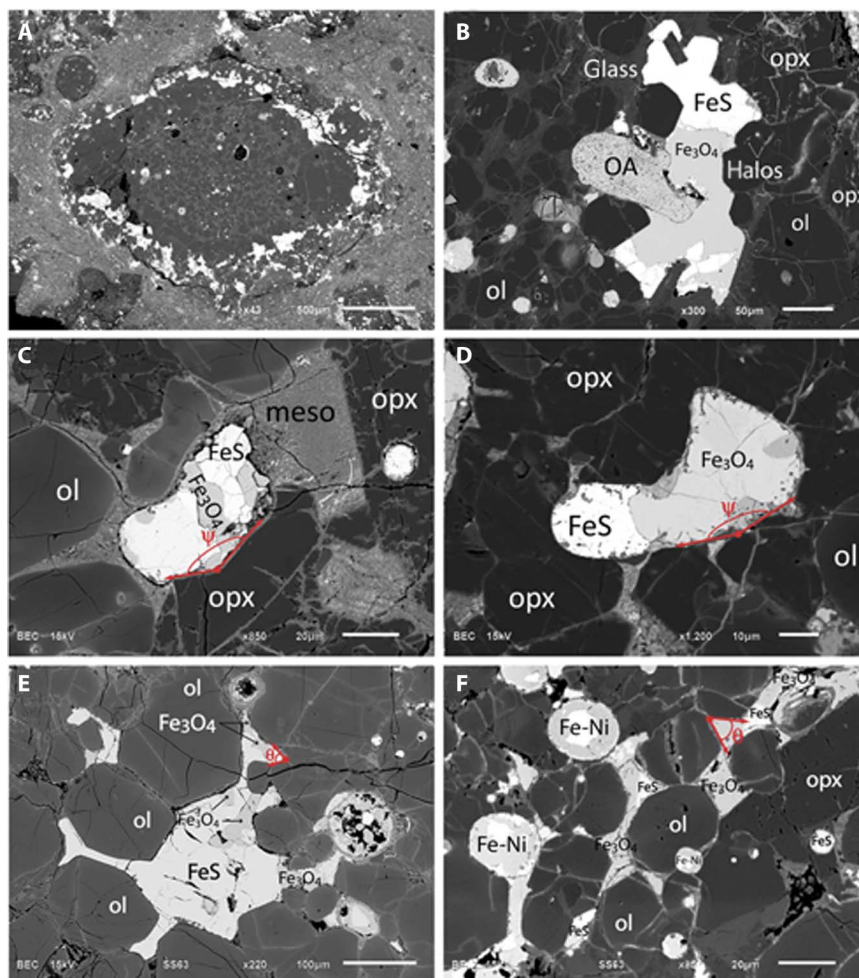*Corresponding author. Email: yvesm@crpg.cnrs-nancy.fr

Fig. 1. Petrographic survey of magnetite-bearing Vigarano-like carbonaceous (CV) chondrules. (**A**) Backscattered electron image of a porphyritic olivine-pyroxene (POP) chondrule in Kaba (CV3) revealing the preferential distribution of sulfides (FeS) and magnetites (Fe_3O_4) in the outer zone mainly composed of low-Ca pyroxenes. (**B**) Ameboidal Fe_3O_4 in contact with olivine, low-Ca pyroxene, and mesostasis (meso) within a chondrule of Vigarano. (**C**) Ameboidal Fe_3O_4 surrounded by mesostasis in Kaba. (**D**) Ameboidal Fe_3O_4 in contact with olivine, low-Ca pyroxene, and mesostasis within a chondrule of Vigarano. (**E**) Liquid-shaped Fe_3O_4 entrapped between olivine in a POP chondrule of Vigarano. A rounded opaque assemblage (OA) is also observed in direct contact with the magnetite. (**F**) Large sulfide-magnetite pool partially entrapping olivine and low-Ca pyroxenes within a chondrule of Vigarano.

Sulfur isotopic compositions are expressed in δ units, per mil (‰) deviations of the $^{34}S/^{32}S$ and $^{33}S/^{32}S$ ratios relative to a standard [here, Vienna-Canyon Diablo Troilite (VCDT)], according to the equation $\delta^{33,34}S = [(^{33,34}S/^{32}S)_{sample}/(^{33,34}S/^{32}S)_{VCDT} - 1] \times 1000$. All sulfides within SAMs [four type I chondrules, three POP, and one porphyritic pyroxene (PP) were studied in detail] show $\delta^{34}S_{VCDT}$ from -1 ± 0.4‰ to $+1.4 \pm 0.4$‰ and $\delta^{33}S_{VCDT}$ from -0.6 ± 0.2‰ to $+0.8 \pm 0.2$‰ (fig. S3 and table S3).

DISCUSSION

Magmatic origin of magnetite
SAMs are Cr-free, devoid of Fe-Ni metal beads, and have textures typical of the crystallization of high-temperature liquids, revealing that they do not result from the oxidation of Cr-bearing Fe-Ni metal beads

(OAs; Fig. 1, B and E, table S1, and fig. S2). This is confirmed by petrographic observations showing that SAMs surrounded by mesostasis (Fig. 1, C and D) present nonwetting angles ($\psi > 90°$, $n = 44$) in contrast with the acute angles ($\theta = 49° \pm 16°$, $n = 26$) observed in silicate melt–free contact between SAMs and olivines/low-Ca pyroxenes (Fig. 1, E and F). This dichotomy is consistent with the formation of SAMs from magmatic FeSO melts. First, sulfide-magnetite associations similar to SAMs have been experimentally produced from FeSO melts generated at various fO_2 (12). Second, experiments have demonstrated that in the absence of silicate melt, the amount of O dissolved in FeS melts has a critical effect on the dihedral angles between silicate minerals and FeSO mattes (13): a transition from nonwetting to wetting behavior (that is, $\theta = 60°$) occurs at around 4 wt % O (fig. S4). In contrast, FeSO melts in contact with silicate melts behave as nonwetting liquids (that is, $\psi > 90°$; Fig. 1) regardless of their oxygen content (fig. S4) (13). Furthermore, SAMs are surrounded by unaltered glassy mesostases

(Fig. 1), inconsistent with an origin via low-temperature aqueous alteration processes, because chondrule glass is prone to alteration by hydrothermal fluids (14). Consequently, the textures and mineralogical compositions of SAMs all demonstrate that they crystallized from FeS melts containing variable amounts of dissolved oxygen segregated from Cr-free chondrule melts.

The oxygen isotopic compositions of SAMs define a linear array with a best-fit slope of 0.933 ± 0.078 (2σ) (Fig. 2), with no indication of mass fractionation [as is expected in the case of aqueous alteration processes; (15)]. This is consistent with the systematic mass-independent oxygen isotopic trend of magnetite in CV chondrules (fig. S5) (16), in contrast with secondary magnetite in chondrules of unequilibrated ordinary chondrites that follow a mass-dependent relationship (fig. S5) (17). Hence, the oxygen isotopic compositions indicate that SAMs are high-temperature magmatic minerals that have recorded the presence of isotopically distinct components in the chondrule-forming region. A high-temperature origin of SAMs is corroborated by their homogeneous sulfur isotopic compositions that agree with a reservoir of chondritic composition (18) and contrast with the much larger $\delta^{34}S_{VCDT}$ variability (from −7 to +6.8‰) reported in CM2 sulfides formed during low-temperature aqueous alteration (fig. S3) (19).

Formation conditions of magmatic magnetite
According to phase diagrams, the formation of FeSO melts in chondrules can only be achieved under oxidizing conditions [reported relative to the Iron-Wüstite (IW) buffer] in the range of IW + 1 to IW + 2 (fig. S6). These fO_2 values are eight to nine log units higher than a gas

of solar composition (Fig. 3), demonstrating the formation of SAM-bearing chondrules under extreme noncanonical conditions. This fO_2 range is also several orders of magnitude higher than that determined for other type I chondrules based on the olivine fayalite contents (20) (Fig. 3). This difference in fO_2 is most likely the result of the complex history of type I chondrules and their precursors. The prominent lack of chemical and oxygen isotopic equilibrium between olivines and chondrule glasses observed in some type I chondrules (21, 22) shows that Mg-rich olivines in these chondrules are relict minerals that have preserved, at least partly, the chemical and isotopic compositions of chondrule precursors. Hence, the fO_2 recorded by type I chondrule olivines is likely to track the conditions that prevailed during the formation of chondrule precursors. In contrast, the much higher oxygen fugacity required for stabilizing FeSO mattes reflects the oxidizing nature of the gas in which the last chondrule-melting event took place. Despite these drastic oxidizing conditions, the relict olivines likely preserved their Mg-rich composition because of the preferential partitioning of iron into sulfides [$D_{FeS/melt} \approx 10$; (10)] and the low iron content of the chondrule melts [0.5 to 3 wt %; (10)]. However, reequilibration under more oxidizing conditions is recorded by the common presence of fayalitic halos around Fe-Ni metal inclusions in Mg-rich olivines of type I chondrules (Fig. 1B). In this scheme, the oxidation and sulfidation of Fe-Ni metal beads into OA are thus contemporaneous with the formation of SAMs, revealing that the last oxidizing chondrule-melting event had a significant influence on chondrule mineralogy.
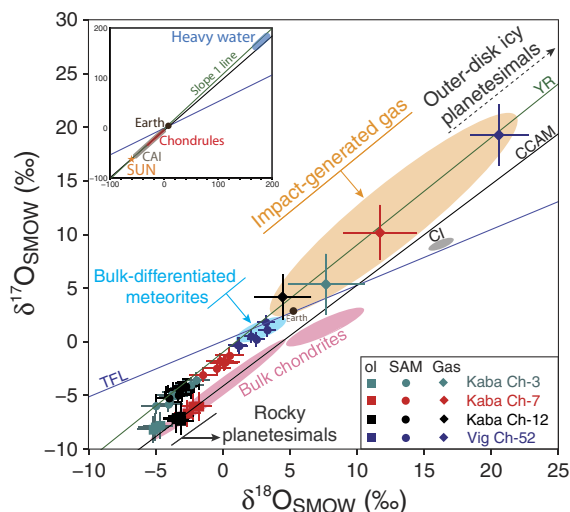

Fig. 2. Oxygen isotopic variations of SAMs and coexisting olivines within chondrules of the Kaba and Vigarano CV3 chondrites. The orange field corresponds to the O-isotopic composition of the impact plume with which the chondrules equilibrated, as modeled (see text) to reproduce the O-isotopic composition of SAMs. There is no meteorite parent body known, either primitive (pink field) or differentiated (blue field), that corresponds to this composition. However, outer-belt icy planetesimals (enriched in ^{17,18}O) would have oxygen isotopic composition corresponding to the impact plume. The inset shows the typical range of oxygen isotopic compositions established for the Sun, CAIs, and chondrules and ice present in meteorites. CCAM, carbonaceous chondrite anhydrous mineral.
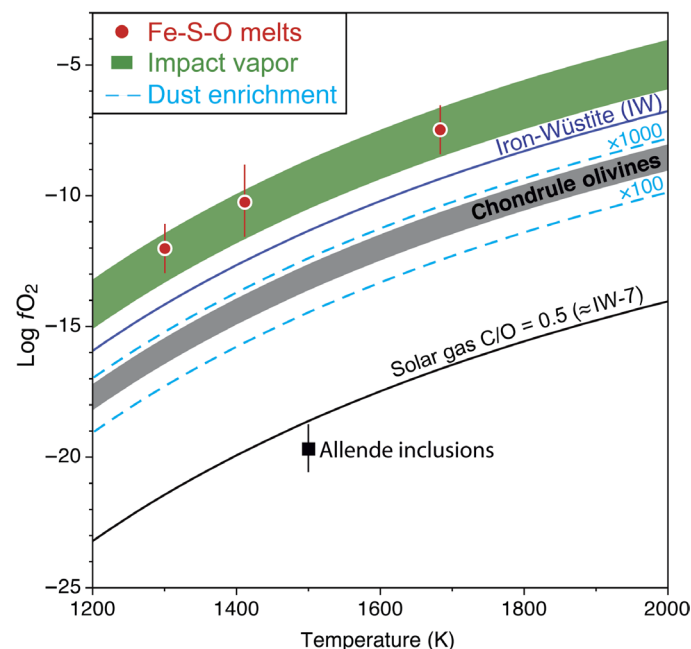

Fig. 3. Conditions of formation of magnetite in CV chondrules. Oxygen fugacity as a function of temperature for a gas of solar composition (C/O = 0.5), the IW buffer, Allende inclusions, and chondrules (as determined from the iron content of olivines in type I chondrules). The fO_2 required for forming and stabilizing FeSO melts (SAMs; red circles) lies ≈3 log units higher than the chondrule olivine field. This fO_2 is in good agreement with that determined for impact-induced silicate melt–vapor plumes (green field).

Formation of chondrules by impact between early generations of planetesimals
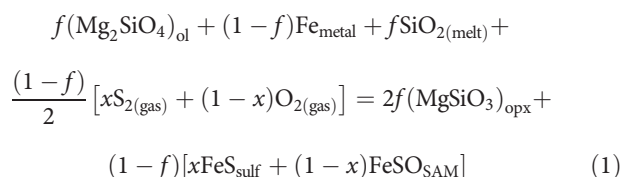
The existence of SAMs in some type I chondrules raises the question of how such oxidizing conditions can be generated in the accretion disk, because a gas of solar composition would be extremely reduced comparatively (that is, IW-7). Although dust enrichments in the nebular gas during chondrule formation enable higher fO_2 (23), these peculiar conditions cannot generate fO_2 higher than IW-2 (Fig. 3) unless invoking dust/gas enrichments in excess of 10^5 to 10^6 that are difficult to produce by any known nebula process. Alternatively, extreme dust enrichment can be easily achieved in impact plumes generated by collisions between planetesimals, thus opening the possibility of producing transient noncanonic gaseous reservoirs (9, 24). Planetesimals are known to have been present in the disk at the time of chondrule formation: Hf/W ages of magmatic iron meteorites and achondrites imply that their parent bodies accreted within the first 0.1 to 0.3 My (25). This is in line with recent numerical simulations of pebble accretion that predict the rapid accretion of 1000-km planetesimals in a few orbital periods due to gravitational instabilities in regions of high dust/gas ratios. Collisions were thus common in the early solar system (26), producing high fO_2 transient impact plumes (24) in good agreement with our estimation inferred from the presence of SAMs within CV chondrules (Fig. 3).

In addition to oxidizing conditions, several lines of evidence suggest chondrule under noncanonical high P_{SiO} (10, 27, 28), imposing important constraints on the conditions of planetesimal collisions, potentially at the origin of chondrules. Dynamical models suggest that two types of impacts between planetesimals occurred during the evolution of the early solar system and could be compatible with the formation of SAM-bearing chondrules: (i) low-velocity impacts induced by dynamical perturbations resulting from the early core formation of giant planets (3) and (ii) high-velocity impacts due to inward-then-outward giant planet migration (29). Although the former do not produce significant vaporization of silicates (30), high P_{SiO} could be achieved by the crystallization of olivine from a magma ocean in partially molten planetesimals (31), with silicate melts enriched in incompatible elements [for example, Si, Al, and Na (32)]. In this scenario, the Mg-rich precursor olivines are likely to be fragments of the impacting bodies that escaped evaporation because of the low velocity of the impacts (30). This would be consistent with the presence in some type I chondrules of olivine-rich clasts having textures, mineralogies, and chemical and isotopic compositions suggesting their possible origin from olivine-dominated differentiated planetesimals (33). In addition, large impact-generated dust enrichments would also imply O-isotopic equilibrium between surviving precursor olivine and newly formed low-Ca pyroxene (22), as commonly observed within porphyritic chondrules (34, 35). Hence, low-velocity impacts could allow (i) the preservation of olivine ± Fe-Ni metal beads as chondrule precursors (36), (ii) the generation of high fO_2 due to extreme dust enrichments, and (iii) the production of high P_{SiO} and P_{Na} as inferred from chondrule mineralogy (9, 37). In this scheme, the accretion of chondrites could be directly related to the chondrule-forming event, as expected from the matrix-chondrule complementary (38). High fO_2 and P_{SiO} would also be a natural consequence of high-velocity impacts between planetesimals formed at different heliocentric distances because of the inward-then-outward gas-driven migration of Jupiter and Saturn in the disk (29). However, one difficulty in this scenario is the fact that high-energy impacts would induce the vaporization of olivines (39), whereas they are present as relict precursors in chondrules (40).

Nature of the impacting bodies at the origin of chondrules

The nature of the impacting bodies, potentially at the origin of SAM-bearing chondrules, can be further constrained from the oxygen isotope systematic. The oxygen isotopic compositions in SAMs and olivines within a given chondrule cannot be related by a mass fractionation process (characterized by a line of slope 0.52 in the three-oxygen isotope diagram; Fig. 2) and thus demonstrate the involvement of several components of different oxygen isotopic compositions in the formation of chondrules. On the basis of the observed petrography and chemical compositions of type I chondrules and their sulfides (10, 41), the formation of SAM-bearing chondrules can be described to the first order by the following reaction

$$f(\mathrm{Mg_2SiO_4})_{ol} + (1-f)\mathrm{Fe}_{metal} + f\mathrm{SiO}_{2(melt)} +$$

$$\frac{(1-f)}{2}\left[x\mathrm{S}_{2(gas)} + (1-x)\mathrm{O}_{2(gas)}\right] = 2f(\mathrm{MgSiO_3})_{opx} +$$

$$(1-f)[x\mathrm{FeS}_{sulf} + (1-x)\mathrm{FeSO}_{SAM}] \qquad (1)$$

where f is the modal abundance of olivine relative to Fe metal and x is the modal abundance of sulfide relative to magnetite in a given chondrule. In this reaction, precursor Mg-rich olivines and Fe-Ni metal are partially molten in volatile-enriched, high fO_2 gas resulting in Si and S enrichment in the chondrule melt and the formation of pyroxene, FeS, and FeSO. Following the approach developed to model the oxygen isotopic compositions of Mg-rich olivines, low-Ca pyroxenes, and mesostases in type I chondrules (22), oxygen isotopic mass balance imposes that (see the Supplementary Materials for details)

$$\delta^{17,18}\mathrm{O}_{gas} = \delta^{17,18}\mathrm{O}_{SAM} - \frac{2f(3\Delta^{17,18}\mathrm{O}_{SAM\text{-}opx} + 2\delta^{17,18}\mathrm{O}_{ol} - 2\delta^{17,18}\mathrm{O}_{SAM})}{(1+f) + x(f-1)} \qquad (2)$$

where $\delta^{17,18}\mathrm{O}_{ol}$ and $\delta^{17,18}\mathrm{O}_{SAM}$ are the oxygen isotope compositions of relict Mg-rich olivine and magnetite in a given chondrule, respectively, and $\Delta^{17,18}\mathrm{O}_{SAM\text{-}opx}$ (that is, $\delta^{17,18}\mathrm{O}_{SAM} - \delta^{17,18}\mathrm{O}_{opx}$) is the equilibrium oxygen isotopic fractionation between SAM and pyroxene. The isotopic compositions of the present SAM-bearing chondrules require a gas composition along the YR line, with $\delta^{18}\mathrm{O}$ and $\delta^{17}\mathrm{O}$ ranging from 4.5 to 20.7‰ and from 4.1 to 19.1‰, respectively (Fig. 2). There is no parent body of any known meteorite that has such a $^{16}\mathrm{O}$-poor oxygen isotopic composition (Fig. 2). However, this composition could well correspond to a plume resulting from the impact between a partially molten planetesimal and an ice-rich planetesimal, or even a cometary object, because nebula ice is thought to be significantly depleted in $^{16}\mathrm{O}$ relative to silicates (42). In this scenario, SAM-bearing chondrules do not represent pristine nebula dust flash-heated in the accretion disk but are by-products of low-velocity collisions between planetesimals early in the history of the solar system.

MATERIALS AND METHODS

Mineralogical and chemical characterization of chondrules

We surveyed all type I chondrules in two thin sections of Vigarano (Vigarano 477-2) and Kaba (Kaba 88-1). Chondrules were examined

microscopically in transmitted and reflected light. Scanning electron microscope observations and energy-dispersive x-ray (EDX) spectral analyses were performed at Centre de Recherches Pétrographiques et Géochimiques (CRPG) using a JEOL JSM-6510 equipped with an EDX Genesis x-ray detector, using a 3-nA primary beam at 15 kV. Quantitative analyses of the mineralogical compositions of chondrules were performed with a CAMECA SX-50 electron microprobe at the University of Paris VI (Camparis facility). A 10-nA focused beam (≈ 2 μm), accelerated to 15-kV potential difference, was used for spot analyses of silicates, oxides, metals, and sulfides with 20-s analysis times. For sulfide analysis, Fe, Ni, Co, and Cr metals, and pyrite and scheibersite were used as standards for Fe, Ni, Co, Cr, S, and P, respectively. Detection limits were estimated at 0.03 atomic % for Fe, Co, and P, 0.08 atomic % for Ni, and 0.006 atomic % for S and Cr. For magnetite analysis, magnetite and chromite were used as standards for Fe, O, and Cr, respectively. Detection limits were estimated at 0.03 atomic % for Fe and O and 0.006 atomic % for Cr. The PAP software was used for matrix corrections.

In both sections of Vigarano and Kaba, all the textural types of chondrules are present [that is, porphyritic olivine (PO), POP, PP, and nonspherical lobate chondrules]. Type I porphyritic chondrules are characterized by small grains of low-FeO olivine (≈ 30 to 100 μm), slightly larger low-Ca pyroxenes (≈ 60 to 150 μm), glassy mesostasis, and Fe-Ni metal beads. Olivines present rounded to subhedral shapes frequently associated with a glassy mesostasis that might contain small Ca-pyroxene crystallites and/or evidence of devitrification. However, the mesostasis does not present any sign of aqueous alteration. Low-Ca pyroxenes are euhedral crystals, with resorbed or poikilitically enclosed olivines and with little mesostasis. Most of these chondrules are radially zoned with olivines and mesostasis located toward the chondrule interiors, whereas the outer zone is dominated by low-Ca pyroxenes parallel to the surface.

Sulfides in type I porphyritic chondrules of Vigarano are present only as stoichiometric troilite blebs (FeS). Most of the sulfide blebs are composed entirely of troilite or are associated with magnetites (SAMs; Fig. 1B) within structures that are devoid of Fe-Ni metal and have textures typical of crystallization from liquids. This is drastically different from the textures of OAs (Fig. 1C) where magnetite is associated with Fe-Ni metal and FeS. Magnetites in OAs are systematically Cr-rich and Fe-poor compared to those in SAMs (fig. S2 and table S1), revealing that SAMs did not form via the oxidation of Cr-rich Fe-Ni metal beads. SAMs are present in all the chondrules, but their distribution is variable. We mainly observed SAMs in association with low-Ca pyroxenes either as massive blebs (10 to 200 μm) or as poikilitically enclosed droplets (10 to 20 μm). In rare cases, SAMs are present in mesostasis pockets as ameboidal sulfide pools (10 to 100 μm) adhering to rounded olivine and low-Ca pyroxene grains and/or to olivine–silicate melt junctions with large obtuse wetting angles. A previous detailed survey using an EDX mapping survey revealed that SAMs are mainly located in the low-Ca pyroxene outer zone and that the amount of SAM increases with the abundance of low-Ca pyroxene. PO chondrules show the lowest SAM concentrations with SAMs being generally located at the periphery of chondrules: PP chondrules present the highest concentration of troilites ± magnetites.

Ion probe measurements (oxygen and sulfur)

Oxygen isotopes. Oxygen isotopic compositions were measured with CAMECA IMS 1280 HR2 at CRPG-CNRS (Nancy, France). $^{16}O^-$,

$^{17}O^-$, and $^{18}O^-$ ions produced by a Cs^+ primary ion beam (~ 10 μm, ~ 250 pA) were measured in multicollection mode with one Faraday cup (FC) for $^{16}O^-$ and two electron multipliers (EMs) for $^{17}O^-$ and $^{18}O^-$. To remove $^{16}OH^-$ interference in the $^{17}O^-$ peak and maximize the flatness of the $^{16}O^-$ and $^{18}O^-$ peaks, entrance and exit slits were adjusted to achieve a mass resolving power of ≈ 7000 for $^{17}O^-$ on the central EM and ≈ 2500 on the off-axis FC and EM. Total measurement time was 420 s (120-s measurement + 300-s presputtering). We used four terrestrial standard materials (San Carlos olivine, magnetite, basaltic glass, and calcite) to (i) define the TFL and (ii) correct the matrix effect on instrumental mass fractionation (IMF) for magnetite and olivine, respectively. The sensitivity of EMs was monitored. Typical count rates obtained on magnetites were 6×10^7 cps for ^{16}O, 2.8×10^4 cps for ^{17}O, and 1.2×10^5 cps for ^{18}O. The 2σ errors were ≈ 1‰ for $\delta^{18}O$, ≈ 0.8‰ for $\delta^{17}O$, and ≈ 1.5‰ for $\Delta^{17}O$. Similar count rates (4.7×10^7 cps for ^{16}O) were obtained on olivines, resulting in similar errors as for magnetites.

Sulfur isotopes. Sulfur isotope compositions were measured on CAMECA IMS 1280 HR2 (CRPG, Nancy, France) by simultaneous measurements of $^{32}S^-$, $^{33}S^-$, and $^{34}S^-$ in multicollection mode with three off-axis FCs. The FCs were intercalibrated before the analytical session to determine their relative gains. A Cs^+ primary beam of 2.5-nA intensity was focused on a spot of ~ 15 μm. Several pyrite and troilite standards were used to determine the IMF and the reference mass discrimination line (allowing $\Delta^{33}S$ to be calculated). Typical $^{32}S^-$ count rates were between 8×10^8 and 2.5×10^9 cps, depending on the sulfide standard analyzed. A typical analysis consists of 2 min of presputtering, followed by data acquisition in 30 cycles of 3 s each. FC backgrounds were measured during the presputtering before each analysis and then used for correcting the data. The 2σ errors achieved under these conditions were ≈ 0.4‰ for $\delta^{34}S$, ≈ 0.2‰ for $\delta^{33}S$, and ≈ 0.5‰ for $\Delta^{33}S$.

SUPPLEMENTARY MATERIALS

Supplementary material for this article is available at http://advances.sciencemag.org/cgi/content/full/2/7/e1601001/DC1

Oxygen mass balance calculation

fig. S1. Compiled EDX maps of Si, Mg, and S of magnetite-bearing chondrules.

fig. S2. Chemical composition of magnetite.

fig. S3. Sulfur isotopic composition of troilite grains associated to magnetite.

fig. S4. Influence of the amount of oxygen dissolved in FeS melts on silicate mineral/Fe-S-O matte dihedral angles.

fig. S5. Three-oxygen isotope diagram showing previous results of oxygen composition of magnetite in CV chondrules.

fig. S6. Fe-S-O phase diagram.

table S1. Chemical composition of magnetite grains.

table S2. Oxygen isotopic composition of magnetite grains.

table S3. Sulfur isotopic composition of sulfides associated to magnetite grains.

References (43–46)

REFERENCES AND NOTES

1. A. W. Howard, Observed properties of extrasolar planets. *Science* **340**, 572–576 (2013).
2. K. Wahlberg Jansson, A. Johansen, Formation of pebble-pile planetesimals. *Astron. Astrophys.* **570**, A47 (2014).
3. K. R. Grazier, J. C. Castillo-Rogez, P. W. Sharp, Dynamical delivery of volatiles to the outer main belt. *Icarus* **232**, 13–21 (2014).
4. R. H. Hewins, Chondrules. *Annu. Rev. Earth Planet Sci.* **25**, 61–83 (1997).
5. S. J. Desch, H. C. Connolly Jr., A model of the thermal processing of particles in solar nebula shocks: Application to the cooling rates of chondrules. *Meteorit. Planet. Sci.* **37**, 183–207 (2002).

6. B. C. Johnson, D. A. Minton, H. J. Melosh, M. T. Zuber, Impact jetting as the origin of chondrules. *Nature* **517**, 339–341 (2015).

7. M. A. Morris, A. C. Boley, S. J. Desch, T. Athanassiadou, Chondrule formation in bow shocks around eccentric planetary embryos. *Astrophys. J.* **752**, 17 (2012).

8. C. M. O'D. Alexander, J. N. Grossman, D. S. Ebel, F. J. Ciesla, The formation conditions of chondrules and chondrites. *Science* **320**, 1617–1619 (2008).

9. A. V. Fedkin, L. Grossman, Vapor saturation of sodium: Key to unlocking the origin of chondrules. *Geochim. Cosmochim. Acta* **112**, 226–250 (2013).

10. Y. Marrocchi, G. Libourel, Sulfur and sulfides in chondrules. *Geochim. Cosmochim. Acta* **119**, 117–136 (2013).

11. E. D. Young, S. S. Russell, Oxygen reservoirs in the early solar nebula inferred from an allende CAI. *Science* **281**, 452–455 (1998).

12. R. O. C. Fonseca, I. H. Campbell, H. St. C. O'Neill, J. D. Fitzgerald, Oxygen solubility and speciation in sulphide-rich mattes. *Geochim. Cosmochim. Acta* **72**, 2619–2635 (2008).

13. G. A. Gaetani, T. L. Groove, Wetting of mantle olivine by sulfide melt: Implications for Re/Os ratios in mantle peridotite and late-satge core formation. *Earth Planet. Sci. Lett.* **169**, 147–163 (1999).

14. Y. Marrocchi, M. Gounelle, I. Blanchard, F. Caste, A. T. Kearsley, The Paris CM chondrite: Secondary minerals and asteroidal processing. *Meteorit. Planet. Sci.* **49**, 1232–1249 (2014).

15. E. D. Young, R. D. Ash, P. England, D. Rumble III, Fluid flow in chondritic parent bodies: Deciphering the compositions of planetesimals. *Science* **286**, 1331–1335 (1999).

16. B.-G. Choi, J. T. Wasson, Microscale oxygen isotopic echange and magnetite formation in the Ningqiang anomalous carbonaceous chondrite. *Geochim. Cosmochim. Acta* **67**, 4655–4660 (2003).

17. B.-G. Choi, K. D. McKeegan, A. N. Krot, J. T. Wasson, Extreme oxygen-isotope compositions in magnetite from unequilibrated ordinary chondrites. *Nature* **392**, 577–579 (1998).

18. X. Gao, M. H. Thiemens, Isotopic composition and concentration of sulfur in carbonaceous chondrites. *Geochim. Cosmochim. Acta* **57**, 3159–3169 (1993).

19. E. S. Bullock, K. D. McKeegan, M. Gounelle, M. M. Grady, S. S. Russell, Sulfur isotopic composition of Fe-Ni sulfide grains in CI and CM carbonaceous chondrites. *Meteorit. Planet. Sci.* **45**, 885–898 (2010).

20. L. Grossman, A. V. Fedkin, S. B. Simon, Formation of the first oxidized iron in the solar system. *Meteorit. Planet. Sci.* **47**, 2160–2169 (2012).

21. M. Chaussidon, G. Libourel, A. N. Krot, Oxygen isotopic constraints on the origin of magnesian chondrules and on the gaseous reservoirs in the early solar system. *Geochim. Cosmochim. Acta* **72**, 1924–1938 (2008).

22. Y. Marrocchi, M. Chaussidon, A systematic for oxygen isotopic variation in meteoritic chondrules. *Earth Planet. Sci. Lett.* **430**, 308–315 (2015).

23. H. Palme, B. J. Fegley Jr., High-temperature condensation of iron-rich olivine in the solar nebula. *Earth Planet. Sci. Lett.* **101**, 180–195 (1990).

24. C. Visscher, B. J. Fegley Jr., Chemistry of impact-generated silicate melt-vapor debris disks. *Astrophys. J.* **767**, L12 (2013).

25. T. S. Kruijer, T. S. Kruijer, M. Touboul, M. Fischer-Gödde, K. R. Bermingham, R. J. Walker, T. Kleine, Protracted core formation and rapid accretion of protoplanets. *Science* **344**, 1150–1154 (2014).

26. D. P. O'Brien, M. V. Sykes, The origin and evolution of the asteroid belt—Implications for Vesta and Ceres. *Space Sci. Rev.* **163**, 41–61 (2011).

27. D. C. Hezel, H. Palme, L. Nasdala, F. E. Brenker, Origin of SiO$_2$-rich components in ordinary chondrites. *Geochim. Cosmochim. Acta* **70**, 1548–1564 (2006).

28. P. Friend, D. C. Hezel, D. Mucerschi, The conditions of chondrule formation, Part II: Open system. *Geochim. Cosmochim. Acta.* **173**, 198–209 (2016).

29. K. J. Walsh, A. Morbidelli, S. N. Raymond, D. P. O'Brien, A. M. Mandell, A low mass for Mars from Jupiter's early gas-driven migration. *Nature* **475**, 206–209 (2011).

30. R. G. Kraus, S. T. Stewart, D. C. Swift, C. A. Bolme, R. F. Smith, S. Hamel, B. D. Hammel, D. K. Spaulding, D. G. Hicks, J. H. Eggert, G. W. Collins, Shock vaporization of silica and the thermodynamics of planetary impact events. *J. Geophys. Res.* **117**, E09009 (2012).

31. F. Faure, L. Tissandier, G. Libourel, R. Mathieu, B. Welsch, Origin of glass inclusions hosted in magnesian porphyritic olivines chondrules: Deciphering planetesimal compositions. *Earth Planet. Sci. Lett.* **319–320**, 1–8 (2012).

32. A. Boujibar, D. Andrault, N. Bolfan-Casanova, M. A. Bouhifd, J. Monteux, Cosmochemical fractionation by collisional erosion during the Earth's accretion. *Nat. Commun.* **6**, 8295 (2015).

33. G. Libourel, M. Chaussidon, Oxygen isotopic constraints on the origin of Mg-rich olivines from chondritic meteorites. *Earth Planet. Sci. Lett.* **301**, 9–21 (2011).

34. T. J. Tenner, D. Nakashima, T. Ushikubo, N. T. Kita, M. K. Weisberg, Oxygen isotope ratios of FeO-poor chondrules in CR3 chondrites: Influence of dust enrichment and H$_2$O during chondrule formation. *Geochim. Cosmochim. Acta* **148**, 228–250 (2015).

35. T. Ushikubo, M. Kimura, N. T. Kita, J. W. Valley, Primordial oxygen isotope reservoirs of the solar nebula recorded in chondrules in Acfer 094 carbonaceous chondrite. *Geochim. Cosmochim. Acta* **90**, 242–264 (2012).

36. G. Libourel, A. N. Krot, Evidence for the presence of planetesimal material among the precursors of magnesian chondrules of nebular origin. *Earth Planet. Sci. Lett.* **254**, 1–8 (2007).

37. A. Kropf, G. Libourel, 42nd Lunar and Planetary Science Conference, LPI Contribution No. 1608, p. 1160.

38. H. Palme, D. C. Hezel, D. S. Ebel, The origin of chondrules: Constraints from matrix composition and matrix-chondrule complementarity. *Earth Planet. Sci. Lett.* **411**, 11–19 (2015).

39. F. Albarede, C. Ballhaus, J. Blichert-Toft, C.-T. Lee, B. Marty, F. Moynier, Q.-Z. Yin, Asteroidal impacts and the origin of terrestrial and lunar volatiles. *Icarus* **222**, 44–52 (2013).

40. R. H. Jones, L. A. Leshin, Y. Guan, Z. D. Sharp, T. Durakiewicz, A. J. Schilk, Oxygen isotope heterogeneity in chondrules from the Mokoia CV3 carbonaceous chondrite. *Geochim. Cosmochim. Acta* **16**, 3423–3438 (2004).

41. G. Libourel, A. Krot, L. Tissandier, Role of gas-melt interaction during chondrule formation. *Earth Planet. Sci. Lett.* **251**, 232–240 (2006).

42. N. Sakamoto, Y. Seto, S. Itoh, K. Kuramoto, K. Fujino, K. Nagashima, A. N. Krot, H. Yurimoto, Remnants of the early solar system water enriched in heavy oxygen isotopes. *Science* **317**, 231–233 (2007).

43. L. Tissandier, G. Libourel, F. Robert, Gas-melt interactions and their bearing on chondrule formation. *Meteorit. Planet. Sci.* **37**, 1377–1389 (2002).

44. T. Chacko, D. R. Cole, J. Horita, in *Stable isotope geochemistry, reviews of mineralogy and geochemistry*, J. W. V. A. R. D. Cole, Ed. (Mineralogical Society of America, Washington, DC, 2001), vol. 43, pp. 1–81.

45. B.-G. Choi, K. D. McKeegan, L. A. Leshin, J. T. Wasson, Origin of magnetite in oxidized CV chondrites: In situ measurement of oxygen isotope compositions of Allende magnetite and olivine. *Earth Planet. Sci. Lett.* **146**, 337–349 (1997).

46. H. Shima, A. J. Naldrett, Solubility of sulfur in an ultramafic melt and the relevance of the system Fe-S-O. *Econ. Geol.* **70**, 960–967 (1975).

Citation: Y. Marrocchi, M. Chaussidon, L. Piani, G. Libourel, Early scattering of the solar protoplanetary disk recorded in meteoritic chondrules. *Sci. Adv.* **2**, e1601001 (2016).